Langmuir

ARTICLE

pubs.acs.org/Langmuir

Efficient Emulsification of Viscous Oils at High Drop Volume Fraction

Slavka Tcholakova,*[,†] Ivan Lesov,[†] Konstantin Golemanov,[†] Nikolai D. Denkov,[†] Sonja Judat,[‡] Robert Engel,[‡] and Thomas Danner[‡]

[†]Department of Chemical Engineering, Faculty of Chemistry, Sofia University, 1164 Sofia, Bulgaria

[‡]BASF SE, Ludwigshafen, Germany

Supporting Information

ABSTRACT: It is shown experimentally in this study that the increase of drop volume fraction can be used as an efficient tool for emulsification of viscous oils in turbulent flow. In a systematic series of experiments, the effects of drop volume fraction and viscosity of the dispersed phase on the mean, d_{32}, and maximum, d_{V95}, diameters of the drops, formed during emulsification, are quantified. The volume fraction, Φ, of the dispersed oily phase is varied between 1% and 90%, and oils with viscosity varying between 3 and 10 000 mPa.s are studied. All experiments are performed at sufficiently high surfactant concentration, as to avoid possible drop−drop coalescence during emulsification. The analysis of the experimental data shows that there is a threshold drop volume fraction, Φ_{TR}, at which a transition from inertial turbulent regime into viscous turbulent regime of emulsification occurs, due to the increased overall viscosity of the emulsion. At $\Phi < \Phi_{TR}$, d_{32} and d_{V95} depend weakly on Φ and are well described by known theoretical expression for emulsification in inertial turbulent regime (Davies, *Chem. Eng. Sci.* **1985**, *40*, 839), which accounts for the effects of oil viscosity and interfacial tension. At $\Phi > \Phi_{TR}$, both d_{32} and polydispersity of the formed emulsions decrease very significantly with the increase of Φ (for the oils with $\eta_D > 10$ mPa.s). Thus, very efficient emulsification of the viscous oils is realized. Very surprisingly, a third regime of emulsification is observed in the range of concentrated emulsions with $\Phi > 75\%$, where the mean drop size and emulsion polydispersity are found experimentally to be very similar for all oils and surfactants studied—an experimental fact that does not comply with any of the existing models of drop breakup during emulsification. Possible mechanistic explanations of this result are discussed. The experimental data for semiconcentrated and concentrated emulsions with $\Phi > \Phi_{TR}$ are described by a simple scaling expression, which accounts for the effects of all main factors studied.

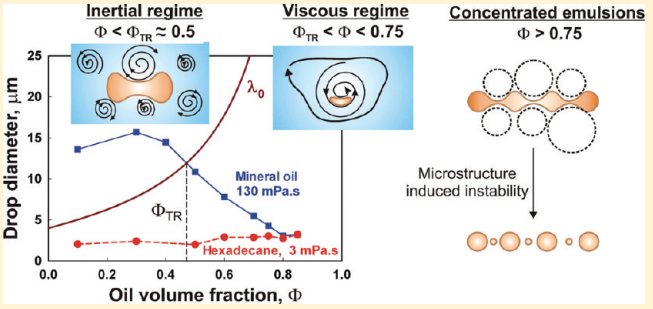

1. INTRODUCTION

The classical studies of the emulsification process in turbulent flow, performed by Kolmogorov[1] and Hinze,[2] showed that two qualitatively different hydrodynamic regimes of drop breakup should be distinguished—breakup in inertial regime of emulsification and breakup in viscous regime of emulsification. In the inertial regime, drop deformation occurs under the action of pressure fluctuations, created by the irregular velocity of the fluid.[1−10] The viscosity of the external phase is of secondary importance in this regime, because the inertial stresses deforming the drops are of nonviscous origin.[1−10] In contrast, drop deformation and breakup in the viscous regime are determined by regular local flows (shear, elongational, etc.) and by the related viscous stresses, which are created by local velocity gradients.[1,2,11−15] In this regime, the viscosity of the continuous phase is an important factor for the efficiency of drop breakup.

In a series of recent studies,[15−17] we studied the effects of several factors (viscosity of the phases, interfacial tension, hydrodynamic conditions, etc.) on the mean drop size and polydispersity of emulsions formed in turbulent flow. An important and nontrivial observation was that the drop size and polydispersity could be strongly reduced (at appropriate conditions) by increasing the viscosity of the external phase, η_C, and/or the drop volume fraction above ca. $\Phi > 40\%$. The latter two effects were explained with the transition from inertial regime of emulsification (at low η_C and Φ) to viscous regime of emulsification (at high η_C and/or high Φ), due to an increase of the size of the smallest turbulent eddies in the turbulent flow (see Figure 1). The latter explanation gave us a conceptual and theoretical framework for analysis of the drop breakup process in concentrated emulsions, subject to turbulent flow.[15]

The focus of the current study is to more deeply analyze the effect of oil volume fraction on the process of drop breakup, especially in the range of semiconcentrated (40 vol % < Φ < 75 vol %) and concentrated emulsions (Φ > 75 vol %). In such emulsions, the interactions between the neighboring drops are very significant and, as a result, the emulsion viscosity could be orders of magnitude higher than the viscosity of the continuous phase.

Received: September 4, 2011
Revised: November 4, 2011
Published: November 05, 2011

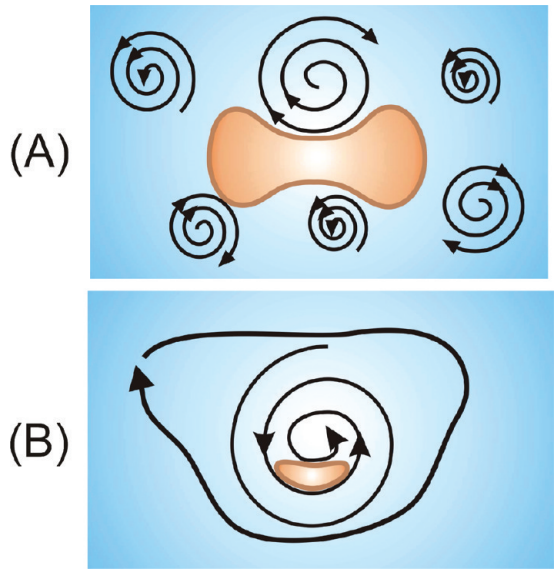

Figure 1. Schematic presentation of the two regimes of emulsification in turbulent flow: (A) Turbulent *inertial* regime—the drops are larger than the smallest turbulent eddies and deform under the action of fluctuations in the hydrodynamic pressure. (B) Turbulent *viscous* regime—the drops are smaller than the smallest turbulent eddies and deform under the action of viscous stress inside and between the eddies.

The drop breakup process in such emulsions is still poorly understood in comparison with the process of drop breakup in diluted emulsions.[1−10] Two main reasons for this scarcity of scientific understanding can be pointed out: (1) Such high volume fractions of the drops usually lead to phase inversion of the emulsions, if inappropriate surfactants are used as emulsion stabilizers.[18−25] (2) The high volume fraction leads to strong and poorly understood dynamic interactions between the drops. The size distribution after drop breakup is strongly affected by these interactions, which makes it difficult (or even impossible) to transfer the knowledge from the experiments with single drops[26−30] to the actual process of emulsification in such systems.

The major aim of the present study is to study systematically and describe quantitatively the effects of drop volume fraction and oil viscosity on the mean, d_{32}, and maximum, d_{V95}, drop sizes in emulsions obtained by rotor-stator homogenizer. For this purpose, we performed systematic experiments, in which the drop size distribution after emulsification at different oil volume fractions, $1\% \le \Phi \le 90\%$, was determined. The emulsions were prepared by two different homogenizers of rotor-stator type, with six different oils as dispersed phase—three mineral oils with viscosity ranging from 3 to 130 mPa.s, and three silicone oils with viscosity between 100 and 10 000 mPa.s. For the emulsions of mineral oils, the role of Φ was studied at three different rotation speeds, with several surfactants giving different interfacial tensions, σ, and within a certain range of viscosities of the continuous phase, η_C. All experiments were performed at high surfactant concentration to avoid drop−drop coalescence during emulsification. Rotor-stator homogenizer was chosen for the study, because this is (probably) the most widely used homogenizer for concentrated emulsions.

The paper is organized as follows: Section 2 summarizes briefly the theoretical expressions from literature for the maximum drop size in emulsions, prepared in the two turbulent regimes of emulsification (inertial and viscous), as well as the main conclusions from the previous studies on drop breakup in sheared liquids or emulsions. Here, we also present expressions for the dependence of emulsion viscosity on drop volume fraction, which are used in Section 5 for data interpretation. Section 3 describes the materials and experimental methods used. Section 4 presents the main results from the emulsification experiments. In Section 5, interpretation of the experimental data is presented. Section 6 summarizes the conclusions.

2. THEORETICAL BACKGROUND

2.1. Maximum Diameter of the Stable Drops in Inertial and Viscous Turbulent Regimes of Emulsification. Drops placed in turbulent continuous phase could break upon the action of viscous or inertial stress, acting on the drop surface. See Figure 1 for an illustration of which of these stresses dominates depending on the ratio of the drop size and the size of the smallest turbulent eddies in the flow. The size of the smallest eddies, λ_0, is given by the so-called "Kolmogorov scale", defined as[1,2]

$$\lambda_0 \approx \varepsilon^{-1/4} \eta_C^{3/4} \rho_C^{-3/4} \tag{1}$$

where η_C is the viscosity and ρ_C is the mass density of the continuous phase, while ε is the rate of energy dissipation per unit mass of the fluid [J/kg.s], which characterizes the intensity of turbulent flow during emulsification. As seen from eq 1, for typical emulsions with $\rho_C \approx 10^3$ kg/m^3, the size of the smallest eddies depends on the viscosity of the continuous phase and on the intensity of the flow only. For semiconcentrated and concentrated emulsions, whose viscosity, η_{EM}, is significantly higher than the viscosity of the continuous phase, one can modify the above expression (as a first-level approximation) by replacing η_C with η_{EM}[15]

$$\lambda_0 \approx \varepsilon^{-1/4} \eta_{EM}^{3/4} \rho_C^{-3/4} \tag{1'}$$

For emulsions showing shear-thinning, η_{EM} should be taken at the appropriate shear rate which characterizes the flow.[15]

In inertial regime of emulsification, the drops break due to fluctuations in the dynamic pressure acting on the drop surface. Therefore, the maximum stable drop diameter, d_D, is estimated by equalizing the dynamic pressure fluctuations in the flow, $\langle \Delta P_T(d) \rangle$, with the capillary pressure, P_C, and the viscous stress inside the breaking drop, which leads to the following equation for the maximum drop diameter:[5]

$$d_D = A_1 \left(1 + A_2 \frac{\eta_D \varepsilon^{1/3} d_D^{1/3}}{\sigma} \right)^{3/5} \sigma^{3/5} \rho_C^{-3/5} \varepsilon^{-2/5} \tag{2}$$

where η_D is viscosity of the dispersed phase, σ is interfacial tension, and $A_{1,2}$ are numerical constants, accounting for the relative contributions of the capillary pressure and viscous dissipation inside the breaking drop, respectively. In our previous study,[15] we found that eq 2 describes rather well the measured maximum drop diameters by volume, d_{V95}, for a wide range of oil viscosities ($3 \le \eta_D < 500$ mPa.s), interfacial tensions ($5 \le \sigma \le 28$ mN/m), and energy dissipation rates ($2.2 \times 10^4 \le \varepsilon \le 9.6 \times 10^5$ J/(kg.s)) for emulsions prepared by narrow-gap homogenizer. The values $A_1 = 0.86$ and $A_2 = 0.37$ were determined as best fit parameters when comparing eq 2 with the entire set of obtained experimental results.

In the case of viscous turbulent emulsification, the drop breakup occurs under the action of the viscous stress, τ_C, inside the smallest turbulent eddies of the continuous phase[1,2] and the maximum

stable drop diameter, d_{KV}, is estimated by comparing τ_C with the drop capillary pressure, thus giving the expression:[1,2,31]

$$d_{KV} = A_3 \varepsilon^{-1/2} \eta_C^{-1/2} \rho_C^{-1/2} \sigma \quad (3)$$

Here, A_3 is a numerical constant which may depend on the viscosity ratio of the fluids, $p = \eta_D/\eta_C$. As seen from eq 3, in the viscous regime of emulsification, the drop size depends significantly on the viscosity of the continuous phase, η_C, whereas this dependence is negligible for the inertial regime of emulsification, cf. eq 2.

2.2. Dependence of Emulsion Viscosity on Oil Volume Fraction. As shown in our previous study,[15] the regime of emulsification in turbulent flow could be changed from inertial to viscous by increasing the viscosity of the continuous phase, which does not affect the drop size in the inertial regime, but increases the size of the smallest eddies; see eq 1. Alternatively, the regime could be changed by increasing the drop volume fraction, which leads to an increase of the overall emulsion viscosity, thus also increasing the size of the smallest eddies.[15] Therefore, for detailed analysis of the effect of oil volume fraction on the drop size during emulsification, it is important to know how the emulsion viscosity depends on Φ. Several models for the dependence of η_{EM} on Φ are briefly discussed below, as described in the literature.

For very diluted emulsions with nearly spherical droplets (low capillary numbers), Taylor[32] determined the emulsion viscosity, $\eta_{EM}(\Phi)$ as

$$\eta_{EM} = \eta_C \left(1 + \frac{5p + 2}{2(p + 1)}\Phi\right) \quad (4)$$

where p is the viscosity ratio. In the derivation of eq 4, the interactions between the neighboring drops are neglected and the comparison of this expression with experimental data[33] showed that it underestimates significantly the emulsion viscosity at $\Phi >$ 2%. This expression converges to the Einstein formula for diluted dispersions of spherical solid particles when the viscosity ratio is $p \gg 1$.

By using a cell model, Yaron and Gal-Or[34] derived the following expression for the viscosity of semiconcentrated emulsions:

$$\eta_{EM} = \eta_C \left[1 + I\left(\Phi^{1/3}, p\right)\Phi\right] \quad (5)$$

where $I(\Phi^{1/3}, p)$ presents the following expression:

$$I(\Phi^{1/3}, p) = \frac{5.5[4\Phi^{7/3} + 10 - 84\Phi^{2/3}/11 + 4(1 - \Phi^{7/3})/p]}{10(1 - \Phi^{10/3}) - 25\Phi(1 - \Phi^{4/3}) + 10(1 - \Phi)(1 - \Phi^{7/3})/p} \quad (6)$$

It was shown that the viscosity of Newtonian emulsions (non-shear-thinning emulsions) can be described relatively well by this model.[33,34] However, more concentrated emulsions may exhibit a detectable shear thinning behavior and are not described well by this model.[33] Note that both models, eqs 4 and 5, do not include the interfacial tension of the drops, because they do not account explicitly for the drop deformation in the flowing emulsions.

For concentrated emulsions with drop volume fraction higher than the close-packed one ($\Phi > 0.75$), the drops inevitably deform and the macroscopic viscous stress can be calculated from the energy dissipated inside the transient planar films, formed between the neighboring drops in the shear flow[35,36]

$$\eta_{EM} \approx \eta_C \left[1.16\mathrm{Ca}^{-0.53}\Phi^{5/6}(\Phi - 0.74)^{0.1}/(1 - \Phi)^{0.5}\right] \quad (7)$$

where $\mathrm{Ca} = \eta_C \dot{\gamma} R_{32}/\sigma$ is the capillary number, R_{32} is the mean volume-surface radius of the droplets, $\dot{\gamma}$ is the shear rate, and σ is the interfacial tension. Equation 7 predicts that the viscous stress in concentrated emulsions is approximately proportional to $\mathrm{Ca}^{1/2}$, which includes the effect of interfacial tension, besides the effects of Φ and η_C. The above equation was verified to describe adequately the rheological behavior of different emulsions and foams at $0.80 \leq \Phi \leq 0.98$.[37−39]

We should emphasize that, for simplicity, we neglect in eq 7 the contribution of the yield stress in the effective emulsion viscosity (only the viscous stress is included). The reason is that we use this equation in Section 5 below for data interpretation at high shear rates only, on the order of 10^4−10^5 s^{-1}, where the contribution of the yield stress to the effective emulsion viscosity is negligible, being 2 orders of magnitude smaller than the effect of viscous friction.

The dependence of emulsion viscosity on drop volume fraction, as calculated by the cell model (eqs 5−6), is shown in SI Figure S1 for $0.1 < \Phi < 0.8$, which is the most important range for our consideration, because the drop−drop interactions become very significant in this range. One sees that the viscosity of the emulsion increases more than 2 orders of magnitude with the increase of Φ, which could lead to transition from inertial to viscous regime of turbulent emulsification, as observed in our previous experiments.[15] That is why in the following subsection we summarize briefly the main results from the literature for the drop breakup in regular shear flow.

2.3. Drop Breakup in Shear Flow. The deformation and breakup of isolated drops, subject to shear flow in viscous fluids, was extensively studied theoretically[40−43] and experimentally.[26−30,40,41,44−48] One of the main conclusions from the studies with single drops is that the drop breakup becomes very difficult when the viscosity ratio is very low, $p \ll 1$, and impossible in laminar shear flow when $p > 4$.

In several papers,[49,50] it was demonstrated that the main results from the single-drop studies could be extended to the breakup of the drops in emulsions with low and moderate drop volume fraction ($\Phi \leq 0.70$) by accounting for the overall viscosity of the emulsion. Namely, the viscosity of the continuous phase, η_C, can be replaced by the emulsion viscosity, η_{EM} (at the respective shear rate, $\dot{\gamma}$), in the scaling relations, i.e., one uses $\mathrm{Ca} = \eta_{EM}\dot{\gamma}R/\sigma$ and $p = \eta_D/\eta_{EM}$ in the system description. Thus, experiments in ref 49 showed that the dependence $\mathrm{Ca}_{CR}(p)$ (so-called "Grace plot" − see Figure 12 below) for drops in a series of emulsions with $\Phi \leq$ 0.70 is similar to that for isolated drops, when using η_{EM} instead of η_C in the consideration. Therefore, in such semiconcentrated emulsions, the effect of interdroplet interactions on drop breakup can be accounted for by the so-called "effective medium approach".[49,50]

Drop breakage in more concentrated emulsions (volume fraction above the sphere close-packing, $\Phi > 74\%$) was studied by several groups.[11−15,51,52] Bibette et al.[51] showed that monodisperse emulsions could be formed by simple shear under appropriate conditions. The experiments with concentrated emulsions demonstrated also[14] that the drop breakup in shear flow could occur even when the viscosity ratio is much higher than unity (up to $p \approx 100$), which is well above the established boundary ($p \approx 4$) for breakup of single drops in simple shear flow of Newtonian continuous phase. Mabille et al.[14] found a relatively weak dependence of Ca_{CR} on p, with $\mathrm{Ca}_{CR} \approx 0.1$ for viscosity ratio $p \approx 1$ (while $\mathrm{Ca}_{CR} \approx 0.3$ for single drops with similar viscosity ratio). These latter results emphasize the nontrivial effects of drop−drop

interactions and the facilitated drop breakage in concentrated emulsions.

In the same direction, we found in our previous study[52] on bubble breakup in foams with $\Phi \approx 0.90$ that $Ca_{CR} \approx 0.40$, which is about 2 orders of magnitude lower than the critical stress for breakup of single bubbles in sheared Newtonian liquids, $Ca_{CR} \approx 25$. This large difference in the critical stress was explained by the strong interaction between neighboring bubbles in densely populated foams, which facilitates bubble subdivision into smaller bubbles. To explain the measured low values of the critical stress, a new type of capillary instability of the breaking bubbles/drops in concentrated foams/emulsions was proposed and discussed (so-called "microstructure induced capillary instability").[52]

As seen from the above brief literature overview, the mechanism and conditions for drop breakup in semiconcentrated and concentrated emulsions are far from clear, even for the simplest case of steady shear flow.

3. MATERIALS AND METHODS

3.1. Materials. Several types of surface-active emulsifiers were used to ensure a wide range of oil−water interfacial tensions. The nonionic surfactants were polyoxyethylene-8 tridecyl ether (denoted hereafter as $C_{13}EO_8$; commercial name Lutensol A8) and polyoxyethylene-20 tridecyl ether (denoted hereafter as $C_{13}EO_{20}$; commercial name Lutensol TO20), both products of BASF. As polymer surfactants, we used polyvinyl alcohol (PVA, commercial name Rhodoviol 25/140, $M_n \approx 12\,600$, $M_w \approx 63\,000$, degree of hydrolysis ~88%) and whey protein concentrate (WPC, trade name AMP 8000, product of Proliant). The emulsifier concentration in the aqueous solutions (10 wt % for the nonionic surfactants, 7 wt % for PVA, and 3 wt % for WPC) was chosen sufficiently high to suppress drop−drop coalescence during emulsification for all oil volume fractions studied. Note that, at high Φ, there is a significant depletion of the surfactant from the aqueous phase, due to the large oil−water interfacial area created in the emulsification process (see, e.g., equation (4) in ref 53), which defines the surfactant amount needed to cover the drop surface at various mean drop diameters and volume fractions. Therefore, such high surfactant concentrations were needed to avoid drop coalescence under all conditions studied. The viscosity and interfacial tension of the solutions, quoted below and used in the data analysis, were all taken after correction for the adsorption-driven depletion of the surfactant from the continuous phase.

All aqueous solutions were prepared with deionized water, which was purified by a Milli-Q Organex system (Millipore). The protein and polymer solutions contained also 0.01 wt % of the antibacterial agent NaN_3 (Riedel-de Haën). Glycerol (99.5% p.a.) was used in some experiments to increase the viscosity of the aqueous phase.

As dispersed phase, we used several oils of different viscosities at 25 °C: hexadecane with $\eta_D = 3.0$ mPa.s (product of Merck); mineral oils with $\eta_D = 25$ (Min25) and 130 mPa.s (Min130), both products of Sigma-Aldrich; and three silicone oils with $\eta_D = 95$, 1024, and 10 000 mPa.s (denoted SilXX, where XX expresses the oil viscosity). The silicone oils (products of Rhodia) were used as received. The mineral oils and hexadecane were purified from surface-active contaminations by passing them through a glass column, filled with Florisil adsorbent.

3.2. Methods for Emulsification. *3.2.1. Emulsification by Ultra Turrax.* This equipment was used in the experiments, aimed to study the effect of oil viscosity in wide range (between 3 and 10 000 mPa.s), in which both mineral and silicone oils were included. All experiments were performed by using the following procedure: (1) The necessary amount of oil was added to the aqueous phase, under continuous stirring by metal spoon, to form an oil−water premix in the form of coarse emulsion. (2) This premix was homogenized by Ultra Turrax (Janke & Kunkel GmbH & Co, IKA-Labortechnik) for 5 min, at the prespecified rotation speed. (3) Samples for measuring the mean drop size and for characterization of the rheological properties of the formed emulsions were taken. Water bath was used for maintaining the temperature during emulsification at $T = 25 \pm 3$ °C.

The rotor radius in the Ultra Turrax head was 5 mm, whereas the stator radius was 5.35 mm, thus forming a gap with width of 350 μm.

3.2.2. Emulsification by Magic Lab. Magic Lab is a lab-scale device for rotor-stator emulsification, produced by IKA Germany. This equipment was used in the experiments with mineral oils only to avoid the equipment contamination by silicone oils. The emulsions were obtained in a two-step process: The first step was the formation of oil−water premix (coarse emulsion). In a beaker containing a given volume of surfactant solution, we poured slowly and carefully the mineral oil, under continuous mild stirring with metal spoon. In this way, we prepared 200 mL of the coarse emulsion. Appropriate volumes of oil and surfactant solution were mixed in this step to obtain the desired oil volume fraction, Φ.

In the second step, the coarse emulsion was poured into the inlet funnel of the Magic Lab apparatus. The emulsion passed several times through the homogenization unit, as a result of pumping the emulsion in a closed circulation loop. During this step, the emulsion in the funnel was constantly stirred to suppress drop creaming and to make sure that the entire emulsion passed through the homogenizer. This emulsification stage continued for 15 min. We used rotor Module 6F, at rotation speeds of 5000, 10 200, and 20 000 rpm. The rotor used has a complex geometry with three concentric high-shear gaps. During operation, the emulsion enters first the inner gap and consecutively passes toward the outer gaps. The dimensions of the gap with the largest diameter, where the highest shear rate is realized, are the following: radius 15 mm and gap-width 200 μm.

During emulsification, the sample temperature increased due to the viscous friction in the operational space of the homogenizer head. To maintain the emulsion temperature within the range 25 ± 3 °C, we cooled the homogenization chamber during the experiment with a cryothermostat (model F31−C, Julabo LaborTechnik GmbH). At the end of the 15 min period of emulsification, the emulsion was pumped out of the Magic Lab for the subsequent determination of the drop-size distribution and for characterization of its rheological properties.

3.3. Determination of Drop Size Distribution. The drop size distribution in the obtained emulsions was determined by video-enhanced optical microscopy.[54,55] The oil drops were observed and recorded in transmitted light with microscope Axioplan (Zeiss, Germany), equipped with objective Epiplan ×50, and connected to a CCD camera and video recorder. The diameters of the recorded oil drops were measured by experienced operator, with custom-made image analysis software. Each droplet was measured individually by the operator, thus avoiding the possible errors in the automated image analysis procedures where the drop clusters could be easily mistaken with individual drops. For each sample, the diameters of at least 1000 drops were measured. For the most polydisperse emulsions, at least three (typically five or four) independent emulsification experiments were performed, thus accumulating data for the diameters of >3000 drops, which is a statistically significant number. The accuracy of these measurements was estimated to be ±0.3 μm.[54]

Two characteristic drop sizes were determined from the measured drop diameters:

The mean volume-surface diameter, d_{32}, defined as

$$d_{32} = \left(\sum_i N_i d_i^3\right) / \left(\sum_i N_i d_i^2\right) \quad (8)$$

where N_i is the number of drops with diameter d_i.

The volume-95 diameter, d_{V95}, which is defined as the diameter for which 95% by volume of the dispersed oil is contained in drops with $d \leq d_{V95}$. This diameter was determined from the measured cumulative size-distribution histograms of the drops in the emulsions studied.

The diameter d_{V95} is used as an experimentally accessible measure of the maximum drop size.[15]

As a characteristic of emulsion polydispersity, we used the ratio d_{V95}/d_{32}, viz., the ratio between the diameter of the largest drops in the emulsion to the volume-surface mean diameter.

3.4. Characterization of the Rheological Properties of the Systems. The rheological properties of the concentrated emulsions ($\Phi \geq 0.8$), prepared by Ultra Turrax or Magic Lab, were determined via parallel plate rheometry with Gemini rotational rheometer (Malvern Instuments, U.K.) at temperature of 25 ± 1 °C, by the following procedure: (1) Sample from the obtained emulsion was placed between the parallel plates of the rheometer. (2) The shear stress was measured as a function of the shear rate, which was changed continuously in the range between 1 and 1000 s^{-1}. Two or three consecutive runs were applied for each sample, at 400 μm gap, to check for the reproducibility of the results. (3) The gap was reduced to 200 μm and two additional runs in the same range of shear rates were made. The results were highly reproducible and no dependence on the gap between the plates was detected, which is evidence for the absence of noticeable effects of wall-slip and other possible artifacts.

The dependence of the total stress on the shear rate for steadily sheared emulsions is described well by the Herschel-Bulkley model, which includes three parameters: yield stress, τ_0; consistency, k; and power-law index, n

$$\tau = \tau_0 + \tau_V(\dot{\gamma}) = \tau_0 + k\dot{\gamma}^n \quad (9)$$

Here, $\dot{\gamma}$ is the applied shear rate, τ is the total shear stress, and τ_V is the viscous (rate dependent) stress. As discussed in the literature,[36−39,56,57] it is very convenient to scale the yield stress and the viscous stress by the drop capillary pressure, $P_C \sim \sigma/R_{32}$, whereas the dimensionless shear rate is adequately represented by the capillary number, Ca

$$\tilde{\tau_0} = \frac{\tau_0}{(\sigma/R_{32})} \quad \tilde{\tau_V} = \frac{\tau_V}{(\sigma/R_{32})} \quad \mathrm{Ca} = \frac{\eta_C \dot{\gamma} R_{32}}{\sigma} \quad (10)$$

Here, $\tilde{\tau}_0$ is dimensionless yield stress, $\tilde{\tau}_V$ is dimensionless viscous stress, and R_{32} is mean volume-surface radius.

It is shown in literature[57] that the dimensionless yield stress is a function of the volume fraction of the dispersed phase, Φ, and of the drop polydispersity. Empirical expressions describing this dependence were proposed by Princen[57] for typical polydisperse emulsions and by Mason et al.[58,59] for monodisperse systems.

We are mostly interested in the emulsion viscosity at high shear rates, like those encountered during emulsification. In our previous studies,[35,36] we developed a theoretical model, which accounts for the dissipated energy inside the emulsion films, formed between the colliding drops in sheared emulsions.[35,36] The following expression for the viscous stress was derived:

$$\tilde{\tau_V} \approx 1.2\Phi^{5/6}\frac{(\Phi - 0.74)^{0.1}}{(1-\Phi)^{0.5}}\,\mathrm{Ca}^{0.47} \quad (11)$$

From the above equations, one can calculate the viscosity of a concentrated emulsion at given shear rate, provided that the material characteristics of the emulsion are known (cf. eq 7).

The viscosities of the used surfactant solutions were measured by capillary viscometer (when the viscosity was below 5 mPa.s) and with rotational viscometer model LVDV-II+Pro (Brookfield, USA) when the viscosity was above 5 mPa.s. The viscosity of the oils was measured by Brookfield rotational viscometer.

3.5. Measurement of Interfacial Tension. The equilibrium oil−water interfacial tension was measured by a drop-shape analysis of pendant oil drops, immersed in the surfactant solutions. The measurements were performed on commercial Drop Shape Analysis system DSA 10 (Krüss GmbH, Hamburg, Germany).

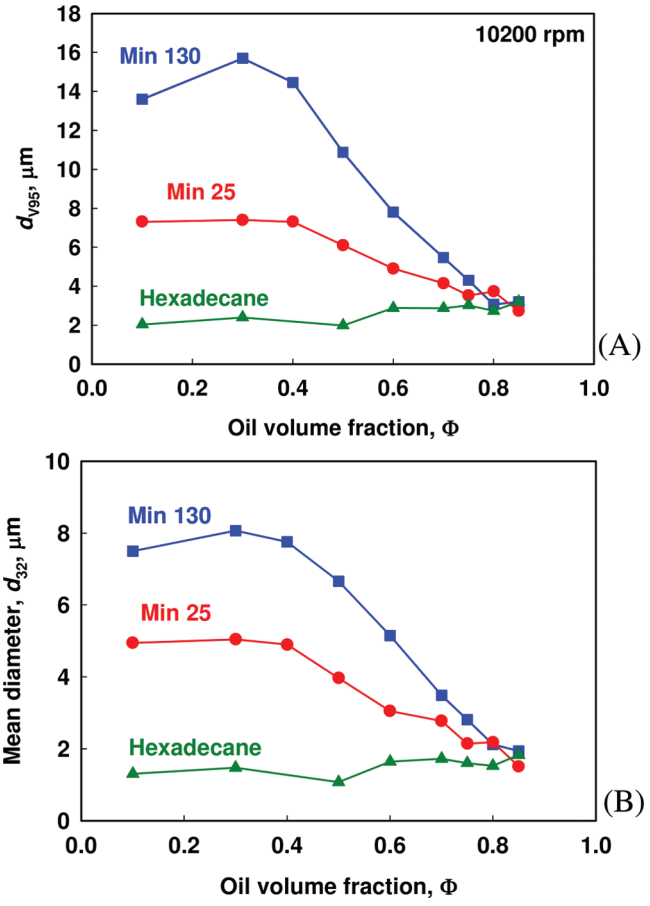

Figure 2. Dependence of (A) maximum drop diameter by volume, d_{V95}, and (B) mean volume-surface diameter, d_{32}, on the oil volume fraction, Φ, for emulsions stabilized by 10 wt % $C_{13}EO_8$ of hexadecane (green triangles), Min25 (red circles), and Min130 (blue squares). These emulsions were prepared by Magic lab homogenizer at 10 200 rpm.

4. MAIN EXPERIMENTAL RESULTS FROM THE EMULSIFICATION EXPERIMENTS

4.1. Effect of Oil Volume Fraction for Mineral Oil Emulsions. The effect of oil volume fraction on the mean drop size, maximum drop size, and polydispersity of the formed emulsions was studied with three mineral oils, having viscosity of 3 mPa.s (hexadecane), 25 mPa.s (Min25), and 130 mPa.s (Min130). As surfactant, in these series of experiments we used 10 wt % $C_{13}EO_8$ with η_C = 4.5 mPa.s and interfacial tension of 2 mN/m for all these oils. All emulsions were prepared by Magic Lab at 10 200 rpm. The temperature was kept at 25 ± 3 °C.

The obtained experimental results are shown in Figure 2. One sees that for Min130 and Min25 emulsions, both d_{32} and d_{V95} remain almost constant at $\Phi \leq 0.4$ and decrease significantly with the increase of Φ from 0.4 to 0.8. The further increase of Φ from 0.8 to 0.85 does not change significantly the mean and maximum drop diameters. On the other hand, the mean and maximum drop diameters in the hexadecane emulsions remain almost constant in the entire range of studied volume fractions; see Figure 2.

This significant decrease in the drop diameters for Min130 and Min25 emulsions, in the intermediate range of oil volume fractions, is accompanied with decrease of emulsion polydispersity from 1.9 to 1.4; see the images in Figure 3. The polydispersity

dx.doi.org/10.1021/la203474b |Langmuir 2011, 27, 14783–14796

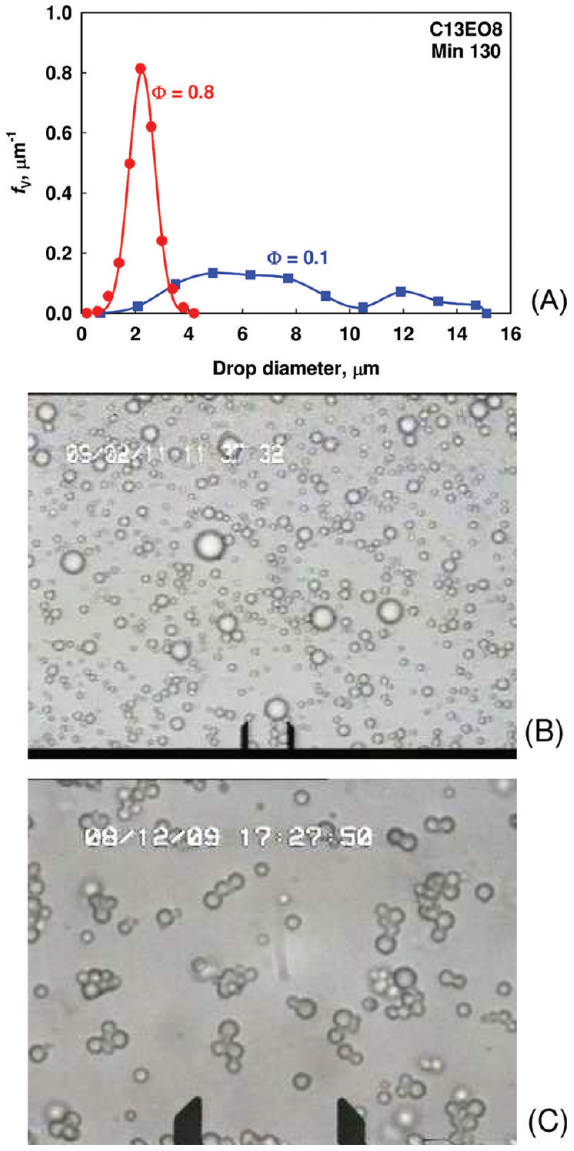

Figure 3. (A) Drop size distribution by volume for Min130 oil-in-water emulsions, formed at $\Phi = 0.1$ (blue squares) and $\Phi = 0.8$ (red circles), stabilized by 10 wt % $C_{13}EO_8$. Representative images from the same emulsions: (B) $\Phi = 0.1$ and (C) $\Phi = 0.8$. The distance between the vertical bars is 20 μm in both images. These emulsions are prepared in Magic lab homogenizer at 10 200 rpm.

here is defined as the ratio between the maximum and mean drop diameters, d_{V95}/d_{32}.

The comparison between the different oils at given drop volume fraction showed that, for emulsions with $\Phi \leq 0.75$, both d_{32} and d_{V95} increase with the increase of η_D. For example, at $\Phi = 0.1$, d_{V95} for Min130 emulsion is around 2 times larger than d_{V95} for Min25 emulsion, which in turn is around 3.5 times larger than d_{V95} for hexadecane emulsions. On the other hand, the effect of η_D decreases with the increase of the oil volume fraction and becomes negligible at $\Phi \approx 0.80$. Remarkably, at such high volume fractions, all emulsions have very similar mean drop diameters (and similar maximum diameters). Furthermore, the drop-size distribution histograms are also similar for the various oils, a fact which is in a sharp contrast with the results obtained at low Φ (see the size-distribution histograms in SI Figure S2).

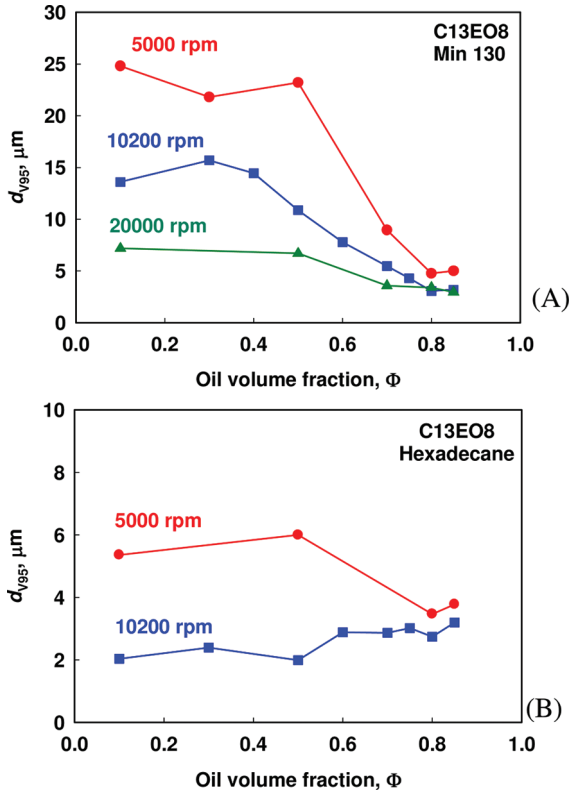

Figure 4. Dependence of the maximum drop diameter by volume, d_{V95}, on the oil volume fraction, Φ, for (A) Min130 and (B) hexadecane in water emulsions, stabilized by 10 wt % $C_{13}EO_8$, prepared in Magic lab at 5000 rpm (red circles), 10 200 rpm (blue squares), and 20 000 rpm (green triangles).

From this series of experiments, we can conclude that the drop size decreases significantly with increasing Φ for emulsions of mineral oils with $\eta_D \geq 25$ mPa.s. For emulsions with $\Phi < 0.8$, the mean and maximum drop sizes increase with η_D, whereas at $\Phi \geq 0.80$, the emulsions formed from all studied mineral oils have $d_{V95} \approx 3$ μm and $d_{32} \approx 1.8$ μm.

4.2. Effect of the Rotation Speed on the Dependence $d(\Phi)$. Experiments at three rotation speeds (5000, 10 200, and 20 000 rpm) were performed with Min130 emulsions, at different oil volume fractions, and the obtained results for d_{V95} are shown in Figure 4A. One sees that the dependences $d(\Phi)$ are similar for all rotation speeds used. At $\Phi \leq 0.4$, d_{V95} almost does not depend on Φ, but depends significantly on the rotation speed—smaller drops are formed at higher rotation speed. At higher volume fraction, $0.4 \leq \Phi < 0.80$, both d_{V95} and d_{32} decrease significantly with increasing Φ. In this range of volume fractions, d_{V95} and d_{32} still depend strongly on the rotation speed. In contrast, at $\Phi \geq 0.80$, the effect of the rotation speed is much smaller, compared to that at lower Φ.

A similar series of experiments was performed with hexadecane emulsions at two rotation speeds: 5000 and 10 200 rpm. One sees from Figure 4B that, at the lower speed, there is a transitional oil volume fraction, $\Phi_{TR} \approx 0.5$, above which the mean and maximum drop sizes in the formed emulsions decrease with the increase of Φ, similar to the case of emulsions with more viscous oils. Therefore, we see that, as observed with the viscous oils, at lower rotation speeds hexadecane reproduces the main trend for the dependence of the drop size on oil volume fraction. At higher rotation speed, a slight increase of the mean and maximum drop

dx.doi.org/10.1021/la203474b |*Langmuir* 2011, 27, 14783–14796

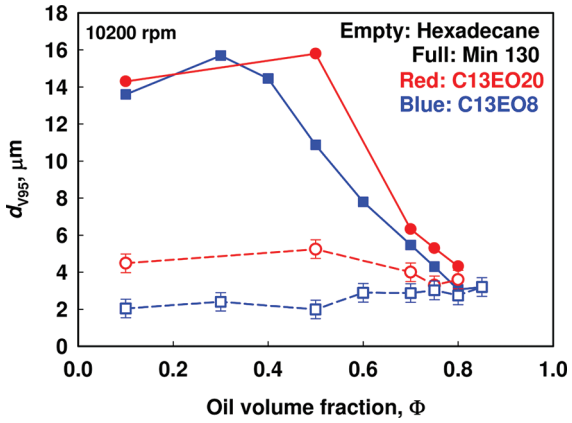

Figure 5. Dependence of the maximum drop diameter by volume, d_{V95}, on the oil volume fraction, Φ, for hexadecane (empty symbols) and Min 130 (full symbols) emulsions, stabilized by 10 wt % of $C_{13}EO_{20}$ (red symbols) and $C_{13}EO_8$ (blue symbols). These emulsions are prepared in Magic lab homogenizer at 10 200 rpm.

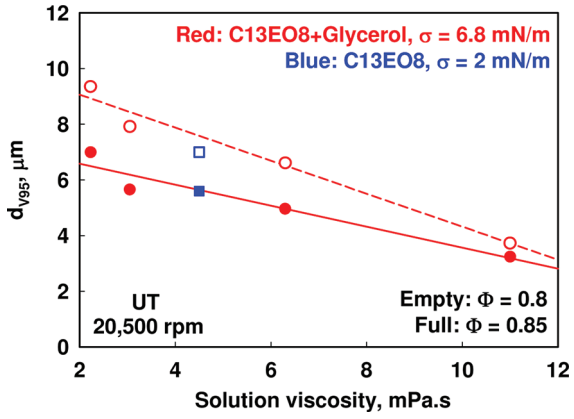

Figure 6. Maximum drop diameter by volume, d_{V95}, as a function of the viscosity of the continuous phase for Min130 oil-in-water emulsions, stabilized by 10 wt % $C_{13}EO_{20}$ + different concentrations of glycerol (red circles) and 10 wt % $C_{13}EO_8$ (blue squares) with oil volume fractions of Φ = 0.80 (empty symbols) and Φ = 0.85 (full symbols). These emulsions were prepared by stirring with Ultra Turrax homogenizer at 20 500 rpm for 5 min.

diameters is seen until they reach the values observed with the more viscous oils, $d_{V95} \approx 3$ μm and $d_{32} \approx 1.8$ μm.

To conclude, the most unexpected result from these experiments is the observation that the effect of the rotation speed is significantly reduced in concentrated emulsions and small droplets are formed with viscous oils, even at moderate speeds.

4.3. Effects of the Interfacial Tension and Viscosity of the Continuous Phase. To check how the surfactants used affect the mean and maximum drop diameters of the formed emulsions, we performed two series of experiments using 10 wt % solutions of $C_{13}EO_8$ (η_C = 4.5 mPa.s and σ = 2.0 mN/m) and $C_{13}EO_{20}$ (η_C = 2.7 mPa.s and σ = 6.8 mN/m). These emulsions were prepared by Magic lab at 10 200 rpm. As oily phases, we used Min130 and hexadecane. The obtained results for Min130 oil emulsions are shown in Figure 5. One sees that the dependences $d(\Phi)$ are very similar for both surfactants, with the mean and maximum drop diameters being slightly larger for emulsions stabilized by $C_{13}EO_{20}$. However, the observed difference is relatively small for all volume fractions studied. This is a nontrivial result, which deserves mechanistic explanation, because the interfacial tensions in these two systems are rather different. From the analysis of the drop breakup process at low Φ, where the emulsification is in the inertial regime (see eq 2), we can deduce that the effect of σ is relatively small for viscous oils, due to the fact that the viscous dissipation inside the breaking drops prevails over the capillary pressure effects—the second term dominates in eq 2. At high Φ, however, where the drop breakup is caused by a combination of viscous and capillary forces, another explanation is needed—see section 5 below.

The experimental results for hexadecane emulsions are also shown in Figure 5. As expected for oil with lower viscosity, the interfacial tension significantly affects the drop size at low Φ, where the emulsification occurs in inertial turbulent regime (the first term in eq 2 is significant). At Φ > 0.5, the transition to viscous regime of emulsification leads to a much smaller effect of interfacial tension on the size of the formed drops.

The experimental results presented above do not allow one to distinguish well between the effects of interfacial tension and those of continuous phase viscosity, because both change when the surfactants are varied. To distinguish between these two effects, we performed an additional series of experiments with 10 wt % $C_{13}EO_{20}$ (σ = 6.8 mN/m) by adding glycerol in the aqueous phase. The added glycerol did not change significantly the interfacial tension but increased η_C from 2.7 to 11 mPa.s. From the results shown in Figure 6 we conclude that d_{V95} decreases significantly with the increase of η_C.

To check further for the effects of interfacial tension and solution viscosities, we performed experiments with silicone oil-in-water emulsions, formed in 7 wt % PVA (η_C = 75 mPa.s and σ = 15 mN/m) and 10 wt % $C_{13}EO_8$ (η_C = 4.5 mPa.s and σ = 2 mN/m), at intermediate range of oil volume fractions between 0.5 and 0.7. The obtained experimental results are shown in SI Figure S3. One sees that d_{V95} is much smaller in the emulsions formed from PVA solutions, compared to those formed from $C_{13}EO_8$ solution, despite the fact that PVA solution has seven times higher interfacial tension. Therefore, the effect of interfacial tension was negligible for these emulsions, compared to the effect of solution viscosity.

Thus, we conclude that the used emulsifier affects significantly the mean and the maximum drop diameters in the emulsions of low-viscosity oils (hexadecane) at $\Phi < \Phi_{TR} \approx 0.4$, as expected, because the drop capillary pressure is opposing the drop deformation and breakage. In contrast, the effect of σ is relatively small (if any) at higher Φ for both viscous and less viscous oils. On the other hand, the effect of the external phase viscosity, η_C, is very significant for all semidiluted and concentrated emulsions studied.

4.4. Effect of Used Homogenizer on *d*(Φ) Dependence. In another series of experiments, we used Ultra Turrax for emulsification. The emulsions were prepared at 20 500 rpm for 5 min. The temperature was kept around 25 °C, by using a water bath. As oily phase, we used Min130, Min25, and hexadecane. As aqueous phase, we used 10 wt % $C_{13}EO_8$.

The obtained results for the dependence of d_{V95} on oil volume fraction are compared in Figure 7 with those obtained by Magic Lab. One sees that the maximum drop diameters for the emulsions prepared by Magic Lab are somewhat smaller than those for emulsions prepared with Ultra Turrax, under otherwise equivalent conditions. This difference is due to the higher rate of energy dissipation in the Magic Lab, as compared to Ultra Turrax

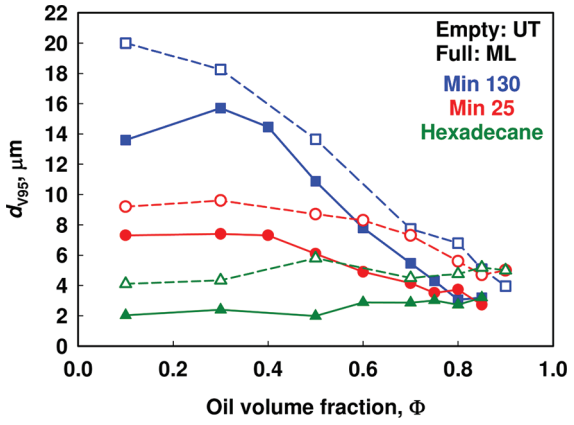

Figure 7. Dependence of the maximum drop diameter by volume, d_{V95}, on the oil volume fraction, Φ, for emulsions stabilized by 10 wt % $C_{13}EO_8$ of Min130 (blue squares), Min25 (red circles), and hexadecane (green triangles), obtained by Ultra Turrax (UT, empty symbols) and Magic Lab (ML, full symbols).

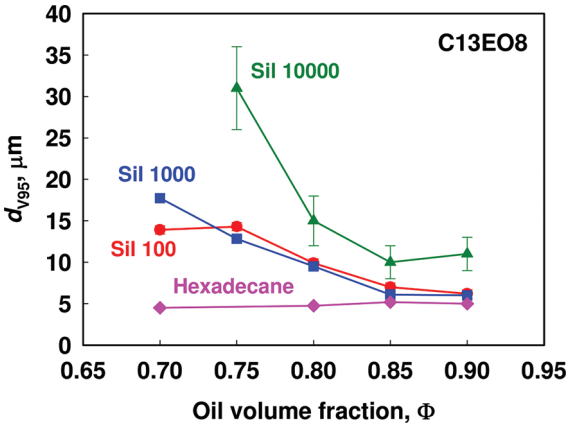

Figure 8. Dependence of the maximum drop diameter by volume, d_{V95}, on the oil volume fraction, Φ, for emulsions of silicone oils with viscosity of 100 mPa.s (red circles), 1000 mPa.s (blue squares), and 10 000 mPa.s (green triangles), all stabilized by 10 wt % $C_{13}EO_8$. These emulsions were prepared by stirring with Ultra Turrax homogenizer at 20 500 rpm for 5 min.

(see Section 5.1 below). Similar dependences were obtained for the mean drop size (data not shown).

However, the most important conclusion from these comparative experiments is that the general trends and the effects of the different factors studied were very similar for the emulsions prepared by the two homogenizers. In particular, at low oil volume fractions, larger and more polydisperse drops are formed when viscous oils are used. In contrast, the mean and maximum drop diameters for all oils are almost the same at $\Phi \geq 0.80$, evidence that the drop breakup process is much less affected by the oil viscosity in the concentrated emulsions.

4.5. Dependence of $d(\Phi)$ for Silicone Oil Emulsions. Silicone oils have the advantage of being available in a much wider viscosity range than the mineral oils. Therefore, we performed additional experiments with silicone oils, with viscosities between 100 and 10 000 mPa.s, by using the procedure described in section 3.2.1. As aqueous phase, in these experiments we used 10 wt % $C_{13}EO_8$ solution. The oil volume fraction was varied between 0.7 and 0.9, because the focus was on the concentrated emulsions.

The obtained experimental results are compared in Figure 8. As in the case of mineral oils, a significant decrease of the drop size is observed with the increase of Φ. The comparison between the different oils shows that, at $\Phi \geq 0.75$, the formed drops of silicone oils with viscosity of 100 and 1000 mPa.s are similar in size and polydispersity. Furthermore, at $\Phi > 0.80$, the results for these oils practically coincide with those obtained with hexadecane (and with the other mineral oils), despite the huge difference in oil viscosity.

The emulsions from silicone oil with viscosity of 10 000 mPa.s are more polydisperse at all studied Φ; however, as with the emulsions of mineral oils, the effect of oil viscosity is much smaller at high Φ.

It should be mentioned that the silicone oil with viscosity 10 000 mPa.s could be emulsified only at sufficiently high volume fraction, $\Phi > 0.70$. Nonemulsified oil was always observed to remain on top of the emulsion during and after emulsification at lower Φ. Therefore, we conclude that we can efficiently emulsify very viscous oils at high Φ, when we choose a proper surfactant for emulsifier. It should be noted that selecting a proper surfactant for emulsification at high Φ is a nontrivial task, and we tested a large set of surfactants to find the emulsifiers described in the current paper.

The most important and unexpected conclusion from this series of experiments is that the viscosity of the oily phase (between 3 mPa.s and 1000 mPa.s) does not affect significantly the mean and maximum drop diameters in emulsions with $\Phi \geq 0.80$. This result certainly reflects some peculiar mechanism of drop breakup in these concentrated emulsions, which has not been discussed in the literature so far—all known models would imply larger effects of oil viscosity and interfacial tension than those observed experimentally.

4.6. Overview of the Main Experimental Results. The main results from all emulsification experiments could be summarized as follows:

(1) When varying the oil volume fraction of the emulsions in wide range, we see three well-defined regions:
- At low drop volume fraction, $\Phi < 0.4$, the drop size distribution depends slightly on Φ, but depends significantly on the viscosity of the two fluid phases and on the rotation speed. For low-viscosity oils, it depends on interfacial tension as well.
- In the intermediate range, $0.4 < \Phi < 0.8$, there is a significant decrease of the drop size and polydispersity with the increase of Φ, for the viscous oils. The dependence of the drop size on the main material parameters are similar to those observed at lower Φ; however, the differences between the various systems gradually disappear with the increase of Φ.
- At high drop volume fractions, $\Phi \geq 0.8$, the drop size and polydispersity depend very weakly on most factors studied (oil viscosity, interfacial tension, speed of rotation), except for the viscosity of the continuous phase—smaller drops are formed at higher η_C.

(2) The dependences $d(\Phi)$ for emulsions prepared in Ultra Turrax and Magic lab are very similar. The only difference is that smaller drops are formed in Magic lab, due to the higher rate of energy dissipation there.

(3) The mineral and silicone oils with similar viscosity give very similar results after emulsification, which shows that

dx.doi.org/10.1021/la203474b |*Langmuir* 2011, 27, 14783–14796

the emulsification is controlled by the general physicochemical variables (viscosities and interfacial tension), without any subtle specific effect of oil chemical composition to be seen.

5. INTERPRETATION OF THE EXPERIMENTAL RESULTS

5.1. Determination of the Average Rate of Energy Dissipation in the Homogenizers. For comparison of the experimental data for d_{V95} with the theoretical predictions for the maximum diameter of the stable drops, one should know the rate of energy dissipation, ε, interfacial tension, σ, and viscosities of the dispersed and continuous phases, η_D and η_C. The values of η_D, η_C, and σ were measured as described in Section 3.

To determine the value of ε in the homogenizers used, we performed a series of experiments with hexadecane in Magic lab and Ultra Turrax. As emulsifier, we used whey protein concentrate (WPC), which provided high interfacial tension, σ = 28.5 mN/m[15] and low viscosity of the continuous phase, η_C = 0.9 mPa.s. Hexadecane was chosen because the viscous dissipation inside the breaking drops is negligible for such oils with low viscosity. Therefore, the drop breakup in these systems occurs in the inertial regime of emulsification and, as shown in our previous study,[15] the experimental data for d_{V95} are described well by the Kolmogorov-Hinze equation, without a need to account for the viscous stress inside the breaking drops:[1,2]

$$d_{KH} = A_1 \sigma^{3/5} \rho_C^{-3/5} \varepsilon^{-2/5} \quad (12)$$

From a series of experiments under various conditions, the value of the numerical constant $A_1 \approx 0.86$, was determined in ref 15.

For the current study, to determine the average value of ε in Ultra Turrax and Magic Lab, we performed a series of experiments at different rotation speeds. It is known from literature that ε depends on the rotation speed, N, and rotor diameter, L, as follows:[7−9]

$$\varepsilon = b_1 N^3 L^2 \quad (13)$$

with values of the numerical constant b_1 found to vary between 1 and 70, depending on the specific geometry of the rotor-stator head.[9,60,61] After introducing eq 13 into eq 12, one obtains

$$d_{KH} = A_1 b_1^{-2/5} \sigma^{3/5} \rho_C^{-3/5} N^{-6/5} L^{-4/5} \quad (14)$$

Equation 14 suggests that the data for d_{V95}, as a function $\sigma^{3/5} \rho_C^{-3/5} N^{-6/5} L^{-4/5}$, should give a straight line that can be used to determine the value of b_1. Using the known values of N, L, and A_1, we determined $b_1 = 40 \pm 4$ for Magic lab and $b_1 = 6 \pm 1$ for Ultra Turrax. These values of b_1 and A_1 are used in all estimates hereafter.

5.2. Regimes of Emulsification and Maximum Drop Size in the Inertial Regime. To determine the regime of emulsification in the various experiments, we compared the size of the largest drops in the system with the size of the smallest eddies, λ_0. As seen from eq 1, the value of λ_0 depends significantly on η_C (or η_{EM} for nondiluted emulsions). Because the emulsion viscosity increases significantly with the oil volume fraction (see SI Figure S1), it could be expected that a transition between the inertial turbulent regime of emulsification and the viscous regime of emulsification should occur at a certain transitional value of Φ, denoted as Φ_{TR} throughout the paper. To estimate the value of Φ_{TR}, we assumed that the viscosity of the emulsion varies according to the model of Yaron and Gal-Or (eq 5) for Φ

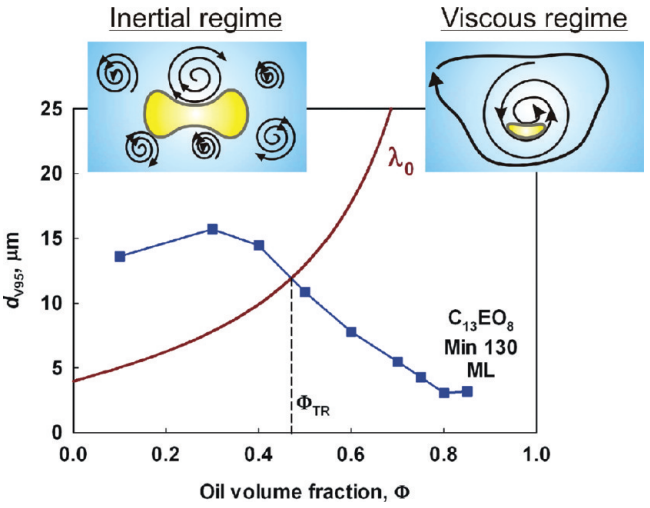

Figure 9. Dependence of the maximum drop diameter by volume, d_{V95}, on the oil volume fraction, Φ, for emulsions of Min130 oil, stabilized by 10 wt % $C_{13}EO_8$ and prepared by stirring in Magic Lab at 10 200 rpm. The brown curve is the theoretically calculated value of λ_0, according to eq 1′ and using eq 5 for calculating η_{EM}.

between 0.1 and 0.8. Then, we can calculate Φ_{TR} by introducing eq 1 into eq 2 and replacing η_C by η_{EM} (given by eq 5). Thus, we obtain the following transcendental equation for Φ_{TR}:

$$I(\Phi_{TR}^{1/3}, p)\Phi_{TR} = 1 - A_3^{4/3}\left(1 + A_4 \frac{\eta_D \varepsilon^{1/4} \eta_C^{1/4} \rho_C^{-1/4} (1 + I(\Phi_{TR}^{1/3}, p)\Phi_{TR})^{1/4}}{\sigma}\right)^{4/5} \frac{\rho_C^{1/5} \sigma^{4/5} \varepsilon^{-1/5}}{\eta_C} \quad (15)$$

where $I(\Phi^{1/3}, p)$ is given by eq 6.

The numerical calculations showed that, at negligible second term in the parentheses (viz., negligible contribution of drop viscosity, which is the case of hexadecane emulsions), the value of Φ_{TR} depends mostly on σ and η_C. For more viscous oils, the transition depends significantly on the viscosity of the dispersed phase as well. The calculated values of Φ_{TR} for the studied systems, under various conditions, are compared in SI Table S1, and some of them are represented in Figure 9.

One sees from SI Table S1 that the hexadecane emulsions, stabilized by $C_{13}EO_8$, are formed under the action of viscous forces, for all hydrodynamic conditions used in our study (with both Magic lab and Ultra Turrax). This is due to the fact that σ is very low (2.0 mN/m) while η_C is relatively high (4.5 mPa.s) in these systems. On the other hand, the hexadecane emulsions stabilized by 10 wt % $C_{13}EO_{20}$ are formed in the inertial regime up to $\Phi_{TR} \approx 0.2$. For Min25 emulsions $\Phi_{TR} \approx 0.1$, while for Min130 emulsions $\Phi_{TR} \approx 0.5$. Thus, we see that it is far from obvious in advance, without more detailed analysis of the operational conditions and material parameters, which of the two regimes of emulsification is realized in a given system.

Summarizing, we can divide all results, presented in section 4, into two major groups: (1) emulsions obtained in inertial regime of turbulent emulsification at $\Phi < \Phi_{TR}$, and (2) emulsions formed in viscous regime of turbulent emulsification at $\Phi > \Phi_{TR}$. For the emulsions formed in the inertial regime, we can compare the experimental results for d_{V95} with the theoretical predictions of eq 2. Such a comparison is made in Figure 10, where we see a very good agreement between the experimentally determined

dx.doi.org/10.1021/la203474b |Langmuir 2011, 27, 14783–14796

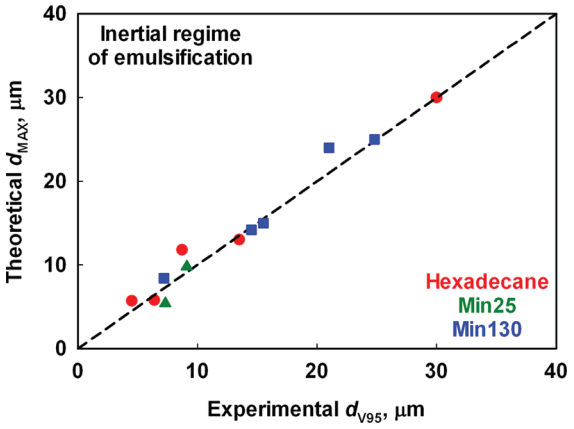

Figure 10. Correlation plot between the experimentally measured values of the maximum stable drop diameter, d_{V95}, for emulsions formed at $\Phi < \Phi_{TR}$ (inertial turbulent regime of emulsification) and theoretically calculated values of d_{MAX} by using eq 2 with numerical constants $A_1 = 0.86$ and $A_2 = 0.18$.

values of d_{V95} and the theoretically calculated values of d_{MAX}. Thus, we conclude that eq 2 describes well the data obtained in the inertial regime of emulsification at $\Phi \leq \Phi_{TR}$.

We should note here that we were forced to use in these estimates $A_2 = 0.18$, instead of $A_2 = 0.37$ (as used in our previous experiments with narrow gap homogenizer), to obtain the good agreement shown in Figure 10. This lower value of A_2 in the current experiments is most probably due to the facts that we used mineral oils and that the emulsion was heated locally in the active zone, due to the high viscous friction there. Thus, we suppose that this local heating decreased significantly the viscosity of the mineral oils in the breaking drops. Indeed, independent measurements of mineral oil viscosity showed rather high temperature dependence—viscosity of Min 130 decreases two times with increasing T from 25 to 40 °C. In contrast, in our previous study we used silicone oils, which are much less sensitive to temperature variations than the mineral oils. Thus, we claim that $A_2 = 0.37$ is the correct physical value, whereas the lower value seen with the mineral oils, $A_2 = 0.18$, compensates for the reduced oil viscosity in the heated active zone of the homogenizer.

5.3. Maximum Drop Size in the Viscous Regime. Our attempt to use eq 3 for interpretation of the data, obtained with emulsions at $\Phi > \Phi_{TR}$, was unsuccessful because the experimental results clearly showed very weak dependence of d_{V95} on σ (see Figure 6), whereas eq 3 predicts that d_{V95} should be proportional to σ. Therefore, eq 3 is inapplicable for description of the experimental data at high oil volume fractions. Note that this equation was successfully used in our previous study[15] to describe the experimental data for d_{V95} on η_C, but for dilute emulsions with $\Phi = 0.01$ only.

Another possible description of the obtained data at $\Phi > \Phi_{TR}$ could be tested by constructing the so-called "Grace plot",[49,50,62] which represents the critical capillary number for the largest stable drops in the formed emulsions, $Ca_{CR} = \eta_{EM}\dot{\gamma}R_{V95}/\sigma$, as a function of the viscosity ratio, $p = \eta_D/\eta_{EM}$. The main idea of the Grace plot is that drops with diameter larger than that corresponding to Ca_{CR}, would be broken into smaller drops by the viscous stress of the sheared medium, whereas the smaller drops would remain unbroken, due to the drop capillary pressure opposing drop deformation. Because we are interested in semiconcentrated and concentrated emulsions, we use here the

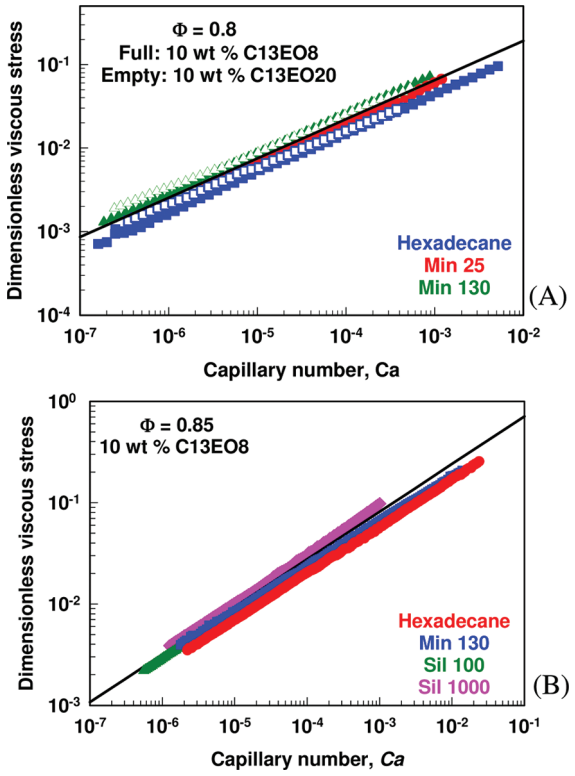

Figure 11. Dimensionless viscous stress, as a function of the capillary number, for emulsions formed at (A) $\Phi = 0.8$ and (B) $\Phi = 0.85$, with different oils and emulsifiers as indicated in the figures. The symbols are experimental data, whereas the lines are drawn according to eq 11.

emulsion viscosity, η_{EM} (instead of η_C), in the definitions of the critical capillary number and viscosity ratio.[49]

To account for the viscosity of the concentrated emulsions, we tested several equations proposed in literature (see section 2). For concentrated emulsions with $\Phi \geq 0.80$, we tested our previous model, describing the viscous stress in steadily sheared emulsions, see eq 7 above.[36,37] To check first whether the emulsions formed in our current experiments are described well by this model, we measured the emulsion rheological characteristics using the procedure described in section 3.4. The obtained results for the emulsions formed at $\Phi = 0.80$ and $\Phi = 0.85$ are compared in Figure 11 with the predictions of eq 11, and a very good agreement is seen. Therefore, eq 7 describes accurately the viscosity of the concentrated emulsions, in the range of shear rates we could test them (up to 10^3 s^{-1}).

Using eq 7, we estimated for the emulsions with $\Phi \geq 0.80$ that the Reynolds number in the gap of the rotor-stator homogenizer is around and below 200 (this number is higher for the emulsions with lower Φ). This estimate suggests that we have no fully developed turbulent flow in the concentrated emulsions and we can use the global shear rate, $\dot{\gamma} = 2\pi rN/l$, for approximate estimates. Here, r is the rotor radius, N is the rotation speed (rotations per second), and l is the gap-width between the rotor and stator. For the Magic lab homogenizer, we thus estimated $\dot{\gamma} \approx 3.9 \times 10^4$ s^{-1}, 8×10^4 s^{-1}, and 1.5×10^5 s^{-1} at 5000, 10 200, and 20 000 rpm, respectively. For Ultra Turrax, we estimated $\dot{\gamma} \approx 3.1 \times 10^4$ s^{-1} as the shear rate at 20 500 rpm.

Thus, we constructed the Grace plot for the studied concentrated emulsions, by using eq 7 for η_{EM} and the global $\dot{\gamma}$, as

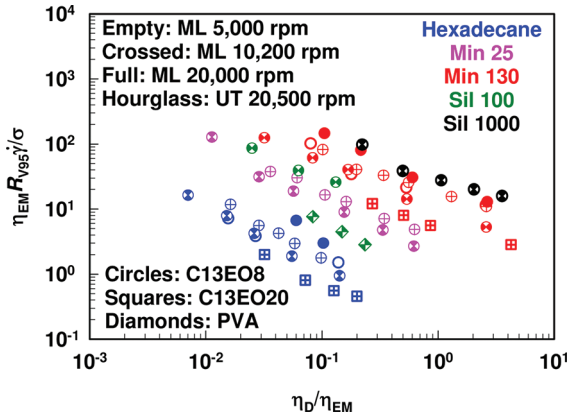

Figure 12. Critical capillary number, $\eta_{EM}\dot{\gamma}R_{V95}/\sigma$, as a function of the viscosity ratio, η_D/η_{EM}, for all emulsions formed at $\Phi > \Phi_{TR}$. The emulsion viscosity, η_{EM}, is calculated by eq 5. ML denotes Magic lab, whereas UT denotes Ultra Turrax homogenizer.

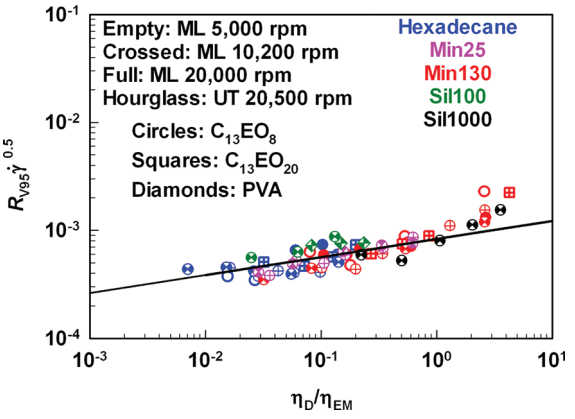

Figure 13. Description of the maximum drop diameter, d_{V95}, by eq 16 for emulsions obtained under various conditions (as shown in the figure), all of them with drop volume fraction $0.4 \leq \Phi \leq 0.9$.

estimated above. One can see from Figure S4 that the scaled experimental data do not fall on a master curve, as the Grace model requires. For example, the experimentally observed weak dependence of the drop size on σ contradicts the requirement $Ca_{CR} \sim 1/\sigma$ (under otherwise equivalent conditions), which is inherent for the Grace plot. Indeed, all data for the emulsions made from $C_{13}EO_{20}$ solutions with $\sigma = 6.8$ mN/m fall well below the data for $C_{13}EO_8$-stabilized emulsions with $\sigma = 2$ mN/m. We tested also several more complex procedures for constructing Grace plots (e.g., using a local shear rate in the turbulent eddies, instead of the global shear rate), but all these attempts were unsuccessful, mainly because they could not capture the observed weak dependence of the maximum drop size in the concentrated emulsions on the interfacial tension and on the rotation speed.

The attempt to construct the Grace plot by using eq 5 for calculating the emulsion viscosity (instead of eq 7) were also unsuccessful; see Figure 12. Again, the data for emulsions with higher surface tension fall well below those obtained with solutions having lower interfacial tension. The effect of rotation speed is also overestimated in this plot. To characterize the local shear flow inside the smallest turbulent eddies, in these estimates we used the relation between the rate of energy dissipation and the local shear rate for non-Newtonian liquids (see eq (17) in ref 15). Nevertheless, we could not scale the data by any of the relations known in the literature.

Concluding, we could not define a self-consistent procedure to represent the experimental data, obtained at $\Phi > \Phi_{TR}$, on appropriate Grace plot, able to merge all data around a single master curve.

Without having other clear theoretical options for data description, we checked whether we could define appropriate scaling law. We found that the experimental results for the mean and maximum drop diameters, obtained at intermediate and high drop volume fraction, $0.4 \leq \Phi \leq 0.85$, could be all described reasonably well by the following formula:

$$d = A\dot{\gamma}^{-0.5}\left(\frac{\eta_D}{\eta_{EM}}\right)^{1/6} \qquad (16)$$

where $A = 1.0 \times 10^{-3}$ for d_{32}, and $A = 1.7 \times 10^{-3}$ for d_{V95}. The emulsion viscosity η_{EM} was calculated by eq 5, and the global shear rate was calculated as explained above.

Figure 13 represents the comparison of the experimental results for all emulsions with $\Phi > \Phi_{TR}$ and the predictions of eq 16. Rather reasonable agreement is observed, taking into account that all parameters are varied in very wide ranges, covering at least 1 order of magnitude for each parameter. Only at very high viscosity ratios, $\eta_D/\eta_{EM} > 20$, do we see more pronounced systematic deviation for two of the points—the experimental radii are about two times larger than the predictions of eq 16. All other data are scattered around the line presenting eq 16, with deviations not exceeding ca. 30%. Thus, we see that the mean and maximum drop diameters depend explicitly on the shear rate and drop viscosity, as well as on drop volume fraction and viscosity of the continuous phase (though η_{EM}). The dependence on η_D and η_C is relatively weak, however, due to the small value of the power-law index in eq 16.

One remarkable feature of eq 16 is the absence of the interfacial tension, which reflects a very unexpected but clear experimental trend—the drop size in the concentrated and semiconcentrated emulsions depended very weakly on σ. This result calls for some mechanistic explanation, because all existing models would require a significant dependence of the drop diameter on the interfacial tension. The main reason for this expectation is the assumption (implicit in all models) that the capillary pressure of the drops opposes their deformation under external viscous stress. Therefore, at fixed external stress, the size of the drops that could be broken increases with σ.

Analyzing the possible reasons for the absence of interfacial tension effect on drop diameter, we found two features of the systems under consideration that could be important in this context (see Figure 14). First, the rotor-stator homogenizers are characterized with complex geometry, which implies sudden changes in the local hydrodynamic flow, e.g., when the emulsion enters and exits the gap between the rotor and the stator, and when flowing around the rotor/stator teeth. From this viewpoint, the actual hydrodynamic flow is much more complex than the regular flows, usually considered in the theoretical models, e.g., when modeling the Grace plot. Such changes in the hydrodynamic conditions were shown experimentally and theoretically[41] to lead to breakage of the drops at smaller aspect ratios than those needed for breakage in steady flows. Therefore, one could expect that the drops could deform in the rotor-stator head up to a given moderate aspect ratio (with small effect of capillary pressure), followed by sudden change of the flow and resulting capillary

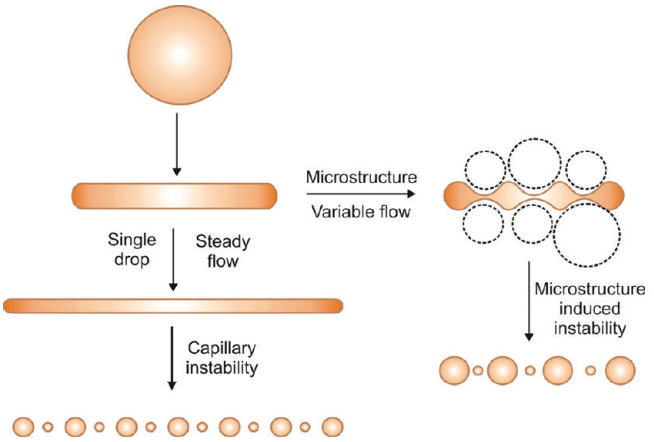

Figure 14. Schematic presentation of the process of single drop breakup in steady flow (left-hand-side images) and of drop breakup in concentrated emulsions and in nonhomogeneous flow (right-hand-side images). For single drops, the breakup occurs when the drop reaches certain critical deformation, which depends on the interfacial tension. In concentrated emulsions and nonsteady shear, the effect of interfacial tension is unclear—the experimental data suggest that this effect is very weak, without clear theoretical explanation of this observation at the present moment.

instability, leading to drop breakup which is not directly controlled by the drop capillary pressure. Second, the interaction with the neighboring drops in the concentrated emulsions could induce capillary instabilities, like those discussed in ref 52 (structure-induced capillary instability), which do not require drop extension up to high aspect ratios. If the neigboring drops induce the actual breakage of the "central" drop, then the effect of interfacial tension on the efficiency of this process is far from clear—on one hand, the higher interfacial tension of the central drop would oppose the deformation of this drop; however, on the other hand, it would also lead to stronger "squeezing" pressure by the neighboring drops, thus facilitating the breakage of the central drop (see Figure 14). To conclude, a much deeper theoretical analysis of the hydrodynamic flow and of the strong effect of the neighboring droplets is needed to reveal the actual reasons for the observed major trends in concentrated emulsions.

6. CONCLUSIONS

We performed a systematic experimental study about the effects of oil viscosity, oil volume fraction, and interfacial tension on the mean and maximum drop diameters in oil-in-water emulsions, prepared in rotor-stator homogenizer. The most important conclusions from the performed study could be summarized as follows:

(1) When varying the drop volume fraction in wide range, we see three well-defined regions (see Figures 2, 4, and 8 for examples):
- At low volume fraction, $\Phi < 0.4$, the drop size distribution depends slightly on Φ, but depends significantly on the viscosity of the two fluid phases, rotation speed, and interfacial tension.
- In the intermediate range, $0.4 < \Phi < 0.8$, there is a significant decrease of drop size and polydispersity with the increase of Φ. The differences between the various systems gradually disappear with the approach of $\Phi \approx 0.8$.
- At high volume fractions, $\Phi \geq 0.8$, the drop size and polydispersity depend very weakly on most factors studied. This regime of emulsification is very appropriate for viscous oils, because drops with small size and low polydispersity are obtained here.

(2) The mineral and silicone oils with comparable viscosity give very similar results after emulsification, which shows that the emulsification is controlled by the general physicochemical variables (viscosities and interfacial tension), without any noticeable effect of the specific chemical composition of the studied oils.

(3) Transition from inertial turbulent to viscous turbulent regime of emulsification is realized at certain value of the drop volume fraction, Φ_{TR} (Figure 9). This value depends on the emulsion material characteristics and on the homogenizer operational conditions, and can be estimated as described in section 5.2.

(4) The results for the emulsions obtained in inertial turbulent regime (at low and moderate drop volume fractions) can be described well by the Kolmogorov-Hinze-Davies approach, with a proper account for the dependence of emulsion viscosity on the drop volume fraction (Figure 10).

(5) Simple scaling law was found to describe all results obtained at moderate and high drop volume fractions, $0.4 \leq \Phi \leq 0.90$ (see eq 16).

The weak dependence of the drop size and polydispersity on the main governing parameters, observed with concentrated emulsions, and the weak dependence of the drop size on interfacial tension for all emulsions with $\Phi > 0.40$, are two rather unexpected results which lack theoretical explanations and call for further experimental and theoretical studies. These observations indicate some specific mechanisms of drop breakup, which are not entirely clear at the present moment (see Figure 14). The available information does not allow us to conclude unambiguously whether these mechanisms are limited to the rotor-stator homogenizers only (like those used in the current study) or they are characteristic for the concentrated emulsions in general. We should emphasize that some of the main trends, observed experimentally in the current study (e.g., the decrease of drop size and polydispersity with the increase of Φ above 0.4 and the efficient homogenization of viscous oils at high Φ) were observed before with the narrow gap homogenizer,[15] which indicates that these trends are general for concentrated emulsions and are not limited to specific homogenizers.

■ ASSOCIATED CONTENT

Supporting Information. Table with calculated threshold drop volume fractions, Φ_{TR}, separating the inertial turbulent regime from the viscous turbulent regime of emulsification. Figure with calculated relative viscosity, η_{EM}/η_C, as a function of oil volume fraction, Φ, calculated by Taylor model,[32] and by Yaron and Gal-Or model.[34] Experimental results for the drop size distribution at $\Phi = 0.1$ and $\Phi = 0.8$ for oils with different viscosities. Experimental results for the maximum drop diameter by volume, d_{V95}, as a function of oil volume fraction, for Sil100 oil-in-water emulsions. Calculated critical capillary number, $\eta_{EM}\dot{\gamma}R_{V95}/\sigma$, as a function of the viscosity ratio, η_D/η_{EM}, for series of emulsions formed at $\Phi = 0.8$ and $\Phi = 0.85$. This material is available free of charge via the Internet at http://pubs.acs.org.

AUTHOR INFORMATION

Corresponding Author

*Assoc. Prof. Slavka Tcholakova, Department of Chemical Engineering, Faculty of Chemistry, Sofia University, 1 James Bourchier Ave., 1164 Sofia, Bulgaria. Phone: (+359-2) 962 5310. Fax: (+359-2) 962 5643. E-mail: SC@LCPE.UNI-SOFIA.BG.

ACKNOWLEDGMENT

The authors gratefully acknowledge the support of this study by BASF. This work is closely related to the activity of COST P21 Action "Physics of Droplets" of the EU.

REFERENCES

(1) Kolmogorov, A. N. Drop breakage in turbulent flow. *Compt. Rend. Acad. Sci. URSS* **1949**, *66*, 825.

(2) Hinze, J. O. Fundamentals of the hydrodynamic mechanism of splitting in dispersion processes. *AIChE J.* **1955**, *1*, 289.

(3) Sprow, F. B. Distribution of drop sizes produced in turbulent liquid-liquid dispersion. *Chem. Eng. Sci.* **1967**, *22*, 435.

(4) Chen, H. T.; Middleman, S. Drop size distribution in agitated liquid-liquid systems. *AIChE J.* **1967**, *13*, 989.

(5) Davies, J. T. Drop sizes of emulsions related to turbulent energy dissipation rates. *Chem. Eng. Sci.* **1985**, *40*, 839.

(6) Lagisetty, J. S.; Das, P. K.; Kumar, R.; Gandhi, K. S. Breakage of viscous and non-Newtonian drops in stirred dispersions. *Chem. Eng. Sci.* **1986**, *41*, 65.

(7) Calabrese, R. V.; Chang, T. P. K.; Dang, P. T. Drop breakup in turbulent stirred-tank contraction. Part I: Effect of dispersed-phase viscosity. *AIChE J.* **1986**, *32*, 657.

(8) Wang, C. Y.; Calabrese, R. V. Drop breakage in turbulent stirred-tank contractors. Part II: Relative influence of viscosity and interfacial tension. *AIChE J.* **1986**, *32*, 667.

(9) Calabrese, R. V.; Wang, C. Y.; Bryner, N. P. Drop breakage in turbulent stirred-tank contractors. Part III: Correlations for mean size and drop size distribution. *AIChE J.* **1986**, *32*, 677.

(10) Berkman, P. D.; Calabrese, R. V. Dispersion of viscous liquids by turbulent flow in a static mixer. *AIChE J.* **1988**, *34*, 602.

(11) Mason, T. G.; Bibette, J. Emulsification in viscoelastic media. *Phys. Rev. Lett.* **1996**, *77*, 3481.

(12) Mason, T. G.; Bibette, J. Shear rupturing of droplets in complex fluids. *Langmuir* **1997**, *13*, 4600.

(13) Jansen, K. M. B.; Agterof, W. G. M.; Mellema, J. Droplet breakup in concentrated emulsions. *J. Rheol.* **2001**, *45*, 227.

(14) Mabille, C.; Leal-Calderon, F.; Bibette, J.; Schmitt, V. Monodisperse fragmentation in emulsions: Mechanisms and kinetics. *Europhys. Lett.* **2003**, *61*, 708.

(15) Vankova, N.; Tcholakova, S.; Denkov, N. D.; Ivanov, I. B.; Vulchev, V.; Danner, T. Emulsification in turbulent flow 1. Mean and maximum drop diameters in inertial and viscous regimes. *J. Colloid Interface Sci.* **2007**, *312*, 363.

(16) Vankova, N.; Tcholakova, S.; Denkov, N. D.; Vulchev, V.; Danner, T. Emulsification in turbulent flow 2. Breakage rate constants. *J. Colloid Interface Sci.* **2007**, *313*, 612.

(17) Tcholakova, S.; Vankova, N.; Denkov, N. D.; Danner, T. Emulsification in turbulent flow 3. Daughter drop-size distribution. *J. Colloid Interface Sci.* **2007**, *310*, 570.

(18) Thakur, R. K.; Villette, C.; Aubry, J. M.; Delaplace, G. Dynamic emulsification and catastrophic phase inversion of lecithin-based emulsions. *Colloids Surf.* **2008**, *315*, 285.

(19) Sajjadi, S. Formation of fine emulsions by emulsification at high viscosity or low interfacial tension: A comparative study. *Colloids Surf.* **2007**, *299*, 73.

(20) Rondon-Gonzaleza, M.; Sadtler, V.; Choplin, L.; Salager, J.-L. Emulsion inversion from abnormal to normal morphology by continuous stirring without internal phase addition: Effect of surfactant mixture fractionation at extreme water−oil ratio. *Colloids Surf.* **2006**, *288*, 151.

(21) Bouchama, F.; van Aken, G. A.; Autin, A. J. E.; Koper, G. J. M. On the mechanism of catastrophic phase inversion in emulsions. *Colloids Surf.* **2003**, *231*, 11.

(22) Sajjadi, S.; Zerfa, M.; Brooks, B. W. Phase inversion in p-xylene/water emulsions with the non-ionic surfactant pair sorbitan monolaurate/polyoxyethylene sorbitan monolaurate (Span 20/Tween 20). *Colloids Surf.* **2003**, *218*, 241.

(23) Sajjadi, S.; Jahanzad, F.; Brooks, B. W. Phase inversion in abnormal O/W/O emulsions: I. Effect of surfactant concentration. *Ind. Eng. Chem. Res.* **2002**, *41*, 6033.

(24) Klahn, J. K.; Janssen, J. J. M.; Vaessen, G. E. J.; de Swart, R.; Agterof, W. G. M. On the escape process during phase inversion of an emulsion. *Colloids Surf.* **2002**, *210*, 167.

(25) Groeneweg, F.; Agterof, W. G. M.; Jaeger, P.; Janssen, J. J. M.; Wieringa, J. A.; Klahn, J. K. On the Mechanism of the Inversion of Emulsions. *Chem. Eng. Res. Des.* **1998**, *376*, 55.

(26) Taylor, G. I. The formation of emulsions in definable fields of flow. *Proc. R. Soc. London, Ser. A* **1934**, *146*, 501.

(27) Tomotika, S. On the instability of a cylindrical thread of viscous liquid surrounded by another viscous fluid. *Proc. R. Soc. London, Ser. A* **1935**, *150*, 322.

(28) Bentley, B. J.; Leal, L. G. A computer-controlled four-roll mill for investigations of particle and drop dynamics in two-dimensional linear shear flows. *J. Fluid Mech.* **1986**, *167*, 219.

(29) Bentley, B. J.; Leal, L. G. An experimental investigation of drop deformation and breakup in steady, two-dimensional linear flows. *J. Fluid Mech.* **1986**, *167*, 241.

(30) Stone, H. A.; Bentley, B. J.; Leal, L. G. An experimental study of transient effects in the breakup of viscous drops. *J. Fluid Mech.* **1986**, *173*, 131.

(31) Cristini, V.; Blawzdziewicz, J.; Loewenberg, M.; Collins, L. R. Breakup in stochastic Stokes flows: sub-Kolmogorov drops in isotropic turbulence. *J. Fluid Mech.* **2003**, *492*, 231.

(32) Taylor, G. I. *Proc. R. Soc. London, Ser. A* **1932**, *138*, 41.

(33) Pal, R. Shear viscosity behavior of emulsions of two immiscible liquids. *J. Colloid Interface Sci.* **2000**, *225*, 359.

(34) Yaron, I.; Gal-Or, B. On viscous flow and effective viscosity of concentrated suspensions and emulsions. *Rheological Acta* **1972**, *11*, 241.

(35) Denkov, N. D.; Tcholakova, S.; Golemanov, K.; Ananthapadmanabhan, K. P.; Lips, A. Viscous friction in foams and concentrated emulsions under steady shear. *Phys. Rev. Lett.* **2008**, *100*, 138301.

(36) Tcholakova, S.; Denkov, N. D.; Golemanov, K.; Ananthapadmanabhan, K. P.; Lips, A. Theoretical model of viscous friction inside steadily sheared foams and concentrated emulsions. *Phys. Rev. E* **2008**, *78*, 011405.

(37) Denkov, N.; Tcholakova, S.; Golemanov, K.; Ananthpadmanabhan, K. P.; Lips, A. Role of surfactant type and bubble surface mobility in foam rheology. *Soft Matter* **2009**, *7*, 3389.

(38) Marze, S.; Langevin, D.; Saint-Jalmes, A. Aqueous foam slip and shear regimes determined by rheometry and multiple light scattering. *J. Rheol.* **2008**, *52*, 1091.

(39) Golemanov, K.; Denkov, N. D.; Tcholakova, S.; Vethamuthu, M.; Lips, A. Surfactant mixtures for control of bubble surface mobility in foam studies. *Langmuir* **2008**, *24*, 9956.

(40) Rallison, J. M. The deformation of small viscous drops and bubbles in shear flows. *Annu. Rev. Fluid Mech.* **1984**, *16*, 45.

(41) Stone, H. A. Dynamics of drop deformation and breakup in viscous fluids. *Annu. Rev. Fluid Mech.* **1994**, *26*, 65.

(42) Hinch, E.; Acrivos, J. A. Steady long slender droplets in two-dimensional straining motion. *J. Fluid Mech.* **1980**, *98*, 305.

(43) Hinch, E. J.; Acrivos, A. Long slender drops in a simple shear flow. *J. Fluid Mech.* **1980**, *98*, 305.

(44) Stone, H. A.; Leal, L. G. The influence of initial deformation on drop breakup in subcritical time-dependent flows at low Reynolds numbers. *J. Fluid Mech.* **1986**, *206*, 223.

(45) Hu, Y. T.; Lips, A. Determination of viscosity from drop deformation. *J. Rheol.* **2001**, *45*, 1453.

(46) Hu, Y. T.; Lips, A. Transient and steady state three-dimensional drop shapes and dimensions under planar extensional flow. *J. Rheol.* **2003**, *47*, 349.
(47) Hu, Y. T.; Lips, A. Estimating surfactant surface coverage and decomposing its effect on drop deformation. *Phys. Rev. Lett.* **2003**, *91*, 044501.
(48) Sibillo, V.; Pasquariello, G.; Simeone, M.; Cristini, V.; Guido, S. Drop deformation in microconfined shear flow. *Phys. Rev. Lett.* **2006**, *97*, 054502.
(49) Jansen, K. M. B.; Agterof, W. G. M.; Mellema, J. Droplet breakup in concentrated emulsions. *J. Rheol.* **2001**, *45*, 227.
(50) Loewenberg, M.; Hinch, E. J. Numerical simulation of a concentrated emulsion in shear flow. *J. Fluid Mech.* **1996**, *321*, 395.
(51) Mabille, C.; Schmitt, V.; Gorria, Ph.; Leal Calderon, F.; Faye, V.; Deminiere, B.; Bibette, J. Rheological and shearing conditions for the preparation of monodisperse emulsions. *Langmuir* **2000**, *16*, 422.
(52) Golemanov, K.; Tcholakova, S.; Denkov, N. D.; Ananthapadmanabhan, K. P.; Lips, A. Breakup of bubbles and drops in steadily sheared foams and concentrated emulsions. *Phys. Rev. E* **2008**, *78*, 051405.
(53) Tcholakova, S; Denkov, N. D.; Danner, T. Role of surfactant type and concentration for the mean drop size during emulsification in turbulent flow. *Langmuir* **2004**, *20*, 7444.
(54) Denkova, P. S.; Tcholakova, S.; Denkov, N. D.; Danov, K. D.; Campbell, B.; Shawl, C.; Kim, D. Evaluation of the precision of drop-size determination in oil/water emulsions by low-resolution NMR spectroscopy. *Langmuir* **2004**, *20*, 11402.
(55) Sather, O. Video-enhanced microscopy investigation of emulsion droplets and size distributions. In *Encyclopedic Handbook of Emulsion Technology*, Sjöblom, J., Ed.; Dekker: New York, 2001; Chapter 15.
(56) Princen, H. M.; Kiss, A. D. Rheology of foams and highly concentrated emulsions: IV. An experimental study of the shear viscosity and yield stress of concentrated emulsions. *J. Colloid Interface Sci.* **1989**, *128*, 176.
(57) Princen, H. M. The structure, mechanics, and rheology of concentrated emulsions and fluid foams. In *Encyclopedia of Emulsion Technology*, Sjöblom, J., Ed.; Marcel Dekker: New York, 2001; Chapter 11, p 243.
(58) Mason, T. G.; Bibette, J.; Weitz, D. A. *J. Colloid Interface Sci.* **1996**, *179*, 439.
(59) Mason, T. G. Rheology of monodisperse emulsions. Ph.D. Thesis; Department of Physics, Princeton University, 1995.
(60) Rushton, J. H.; Costich, E. W.; Everett, H. J. Power characteristics of mixing impellers Part 1. *Chem. Eng. Progress* **1950**, *46*, 395.
(61) Coulaloglou, C. A.; Tavlarides, L. L. Description of interaction processes in agitated liquid-liquid dispersions. *Chem. Eng. Sci.* **1977**, *32*, 1289.
(62) Grace, H. P. Dispersion phenomena in high viscosity immiscible fluid systems and application of static mixers as dispersion devices in such systems. *Chem. Eng. Commun.* **1982**, *14*, 225.